

University of Wollongong
Research Online

Faculty of Engineering and Information
Sciences - Papers: Part A

Faculty of Engineering and Information
Sciences

1-1-2015

**Effect of temperature on microstructure and deformation mechanism of
Fe-30Mn-3Si-4Al TWIP steel at strain rate of 700 s⁻¹**

Zhiping Xiong
University of Wollongong, zx868@uowmail.edu.au

Xue-Ping Ren
University of Science And Technology Beijing


Jian Shu
University of Science And Technology Beijing

Zhe-Lei Wang
University of Science And Technology Beijing

Wei-Ping Bao
University of Science And Technology Beijing

See next page for additional authors

Follow this and additional works at: <https://ro.uow.edu.au/eispapers>

 Part of the [Engineering Commons](#), and the [Science and Technology Studies Commons](#)

Recommended Citation

Xiong, Zhiping; Ren, Xue-Ping; Shu, Jian; Wang, Zhe-Lei; Bao, Wei-Ping; and Li, Shu-Xia, "Effect of temperature on microstructure and deformation mechanism of Fe-30Mn-3Si-4Al TWIP steel at strain rate of 700 s⁻¹" (2015). *Faculty of Engineering and Information Sciences - Papers: Part A*. 3941.
<https://ro.uow.edu.au/eispapers/3941>

Research Online is the open access institutional repository for the University of Wollongong. For further information contact the UOW Library: research-pubs@uow.edu.au

Effect of temperature on microstructure and deformation mechanism of Fe-30Mn-3Si-4Al TWIP steel at strain rate of 700 s⁻¹

Abstract

As twinning-induced plasticity (TWIP) steel is one potential material for shaped charge liner due to the combination of high strength and high plasticity, deformation mechanism at high strain rate and high temperature is required to study. Compression experiments of Fe-30Mn-3Si-4Al TWIP steel were conducted using a Gleeble-1500 thermal simulation machine and a split-Hopkinson pressure bar (SHPB) between 298 and 1073 K at strain rates of 10⁻³ and 700 s⁻¹, respectively. Microstructures were observed using optical microscopy (OM) and transmission electron microscopy (TEM). Results show that flow stress and densities of deformation twins and dislocations decrease with increasing deformation temperature at strain rates of 10⁻³ and 700 s⁻¹. The stack fault energy (SFE) values (Γ) of Fe-30Mn-3Si-4Al TWIP steel at different temperatures were calculated using thermodynamic data. Based on corresponding microstructures, it can be inferred that at 700 s⁻¹, twinning is the main deformation mechanism at 298-573 K for $30 \text{ mJ/m}^2 \leq \Gamma \leq 63 \text{ mJ/m}^2$, while dislocation gliding is the main deformation mechanism above 1073 K for $\Gamma \geq 145 \text{ mJ/m}^2$. In addition, with increasing strain rate from 10⁻³ to 700 s⁻¹, the SFE range of twinning is enlarged and the SEF value of twinning becomes higher.

Keywords

700, 1, 3si, fe, mechanism, deformation, effect, temperature, microstructure, 30mn, 4al, twip, steel, strain, rate

Disciplines

Engineering | Science and Technology Studies

Publication Details

Xiong, Z., Ren, X., Shu, J., Wang, Z., Bao, W. & Li, S. (2015). Effect of temperature on microstructure and deformation mechanism of Fe-30Mn-3Si-4Al TWIP steel at strain rate of 700 s⁻¹. *Journal of Iron and Steel Research International*, 22 (2), 179-184.

Authors

Zhiping Xiong, Xue-Ping Ren, Jian Shu, Zhe-Lei Wang, Wei-Ping Bao, and Shu-Xia Li

Effect of Temperature on Microstructure and Deformation Mechanism of Fe-30Mn-3Si-4Al TWIP Steel at 700 s⁻¹ Strain Rate

XIONG Zhi-ping^{a, b*}, REN Xue-ping^a, SHU Jian^a, WANG Zhe-lei^a,

BAO Wei-ping^c, LI Shu-xia^a

^a School of Materials Science and Engineering, University of Science and Technology Beijing, Beijing 100083, P.R. China;

^b School of Mechanical, Materials and Mechatronic Engineering, University of Wollongong, New South Wales 2522, Australia

^c School of Metallurgical and Ecological Engineering, University of Science and Technology Beijing, Beijing 100083, China

***Corresponding author** Tel: (86)-10-82376475; Fax: (86)-10-62334559

E-mail: zuileniwota@126.com

Abstract: As TWIP steel is one potential metal for Shaped Charge Liner due to the combination of high strength and high plasticity, deformation mechanism under high strain rate and high temperature is studied in this paper. Compression experiments of Fe-30Mn-3Si-4Al TWIP steel were conducted by Gleeble-1500 thermal simulation machine and SHPB (split Hopkinson pressure bar) under 298, 573, 773, 973 and 1073K at 10⁻³ and 700 s⁻¹ respectively. Microstructure evolution with temperature was researched. Effect of strain rate and stack fault energy (SFE) on deformation mechanism was analyzed. Results show that flow stress and densities of deformation twins and dislocations decrease with increasing deformation temperature both at 700 and 10⁻³ s⁻¹. Through thermodynamic calculation, the SFE values (Γ) of Fe-30Mn-3Si-4Al TWIP steel at different temperatures were obtained. Considering microstructures observed by OM and TEM, it can be inferred that at 700 s⁻¹ for $30 \text{ mJ/m}^2 \leq \Gamma \leq 63 \text{ mJ/m}^2$ between 298 and 573 K, twinning is the main deformation mechanism while for $\Gamma \geq 145 \text{ mJ/m}^2$ above 1073 K, dislocation gliding is the main deformation mechanism. Moreover, with increasing strain rate from 10⁻³ to 700 s⁻¹,

the SFE value range for twinning shifts forwards and becomes larger.

Keywords: TWIP steel; Stack fault energy; Deformation mechanism; Dynamic compressive property

1 Introduction

TWIP steel was found when Grässel researched high manganese steel in 1977 [1]. TWIP steel combines high strength and high plasticity, which is one kind of potential steel for Shaped Charge Liner. Deformation mechanism changing from TRIP effect to TWIP effect is due to the SFE increment. Through adjusting chemical component and temperature, the SFE can be adjusted in order to control deformation mechanism [2-4].

With decreasing the SFE, deformation mechanism in quasi-static or static conditions undergoes three stages as follows [5-9]: (i) dislocation gliding stage; (ii) deformation twinning and dislocation gliding stage, which makes high strength and high plasticity coexist and provides the best work hardening rate; (iii) ε or α' martensitic transformations stage, which leads high yield strengths and high work hardening rate. Under quasi-static or static condition, Allain et al. [2] researched Fe-Mn-C austenitic alloys and found that for $\Gamma < 18 \text{ mJ/m}^2$, ε -martensite transformation occurs while for $12 \text{ mJ/m}^2 < \Gamma < 35 \text{ mJ/m}^2$, deformation twinning occurs; Wang et al. [3] studied Fe-25Mn-3Si-3Al TWIP steel and discovered that for $21 \text{ mJ/m}^2 \cong \Gamma \cong 34 \text{ mJ/m}^2$, deformation twinning is the main deformation mechanism, while for $34 \text{ mJ/m}^2 < \Gamma < 76 \text{ mJ/m}^2$, the competition between deformation twinning and dislocation gliding is the main deformation mechanism, while for $\Gamma \cong 76 \text{ mJ/m}^2$ dislocation gliding is the main deformation mechanism. In a word, though adjusting the SFE, deformation mechanism can be controlled in order to obtain different mechanical properties and achieve practical application.

At present, there are few researches on the effect of temperature and SFE on deformation mechanism [2-4]. In addition, it is only involved in quasi-static or static conditions and there is no report regarding influence of high temperature and SFE on deformation mechanism under high strain rate. It is important for using TWIP steel in Shaped Charge Liner to study mechanical properties under high strain rate and temperatures. In this paper, mechanical properties and microstructures under

298~1073K at quasi-static condition (10^{-3} s^{-1}) and high strain rate (700 s^{-1}) were both studied. Though thermodynamic calculation, the SFE values (γ) of Fe-30Mn-3Si-4Al TWIP steel at different temperatures were obtained. According to microstructures observed by OM and TEM, the relation between SFE and deformation mechanism at 10^{-3} and 700 s^{-1} was analyzed. Furthermore, effect of strain rate on deformation mechanism was studied.

2 Experimental materials and methods

TWIP steel used in present study was prepared by induction-melting in an argon atmosphere, and the chemical composition (wt. %) of the steel is as follows: 29.5 Mn, 3.5 Si, 2.94 Al, 0.06 C, 0.006 P, 0.005 S and the bal. Fe. Ingots were solution treated at 1373 K for 2 h, and then forged into bars of around 30 mm in diameter at 1373 K with dry quenching. Then the heat treatment at 1373K for 60 mins then water quenched was conducted after forging. In our previous paper, Fe-30Mn-3Si-4Al TWIP steel can obtain largest elongation with medium strength [10], which is a good condition for applying to Shaped Charge Liner. Samples with 6 mm in diameter and 5 mm in length and 10 mm in diameter and 8 mm in length were cut along the bar axis using wire-electrode cutting method.

Compression experiments were conducted by Gleeble-1500 thermal simulation machine and split-Hopkinson pressure bar under 298, 573, 773, 973 and 1073K at 700 and 10^{-3} s^{-1} respectively. The set of SHPB is illustrated by Ref [10]. Samples were polished by using silicon carbide papers before tests in order to obtain certain depth of parallelism and degree of roughness (Ra.12). To reduce the friction force during experiments, a high pressure lubricant was put on the loading surfaces of samples. For each condition, at least three samples were conducted.

Deformed samples were cut separately along the axis. Microstructures were characterized using an optical microscopy (OM) after mechanical polishing and etching in a 5 vol.% nital and a transmission electron microscope (TEM) operating at 200 kV. Thin foils were prepared by the twin-jet polishing technique using a mixture

of 5 vol.% perchloric acid and 95 vol.% alcohol at 253K with an applied potential of 25 V.

3 Results

3.1 Mechanical properties

Figure 1 shows true strain-stress curves at 10^{-3} and 700 s^{-1} under 298, 573, 773, 973 and 1073 K respectively. At 10^{-3} s^{-1} as shown in Figure 1a, flow stress decreases with temperature increasing from 298 to 773 K, but the decrement becomes smaller. With temperature up to 973 and 1073 K, flow stress first increases abruptly with strain and then gets into a stable state. At 700 s^{-1} as shown in Figure 1b, flow stress decreases with temperature, but the decrement becomes smaller, while peak true strain increases with temperature. In conclusion, flow stress decreases with temperature either at 10^{-3} or 700 s^{-1} .

3.2 Microstructures observation

Microstructures at 10^{-3} s^{-1} under different temperatures were shown in Figure 2. It can be seen that there are many deformation twins between 298 and 773 K as shown in Figure 2a, 2b and 2c, and the density of deformation twins decreases with temperature. With temperature up to 973 K, there are almost no deformation twins and many annealing twins are observed as shown in Figure 2d. Further increasing temperature to 1073 K, there are some recrystallization grains along grain boundaries as shown in Figure 2e. In a word, the density of deformation twins decreases with temperature at 10^{-3} s^{-1} .

Microstructures at 700 s^{-1} under different temperatures were shown in Figure 3. It can be seen that a few annealing twins are retained and deformation twinning does not always depend on annealing twins [11, 12] as shown by lower left red box in Figure 3b. From 298 to 573K, there are some deformation twins. But with temperature increasing from 773 to 1073 K, deformation twins decreases obviously and there are few deformation twins as shown in Figure 3c, 3d and 3e. In a word, the density of deformation twins becomes smaller and smaller with temperature at 700 s^{-1} .

Dislocation configurations under different temperatures at 700 s^{-1} were shown in Figure 4. At 298 K, parallel dislocations were observed while at 573 K, dislocations are entangled and short stack faults (SFs) are observed as illustrated by white arrows in Figure 4b. With temperature up to 773 K, dislocation cells are observed as shown in Figure 4c, whose length is about 2500 nm. Further increasing temperature to 973 K, subgrains exist. In conclusion, dynamic recovery is enhanced while dislocation reactions, dislocation motions and dislocation tangles are strengthened with temperature, resulting in the formation of dislocation cells. With temperature further increasing, dislocation cells and entangled dislocations can form subgrains by dynamic recovery.

Deformation twins under different temperatures at 700 s^{-1} were shown in Figure 5. At 298 K, there are many deformation twins whose spacing is small while from 573 to 973 K, the density of deformation twins become smaller, whose spacing becomes larger. With temperature up to 1073 K, the growth of deformation twins is not sufficient as shown in Figure 5e. In a word, the density of deformation twins and their thickness decrease while their spacing increases with temperature. Moreover, the density of dislocations locating between deformation twins decreases with temperature.

Deformation bands in Figure 2 and Figure 3 consist of deformation twins and dislocations and mainly consist of deformation twins, which are demonstrated by TEM observation in this paper and Ref [3, 13-15]. The density of deformation bands decreases with temperature. It accords with Figure 5 showing that the density of deformation twins decrease with temperature. Deformation twins grow from grain boundaries, which divide the grains into some parts as shown in Figure 3a, 3b and 3c. In fact, deformation twins play an important role like subgrain boundaries in strengthening the materials, which hinder dislocation gliding, resulting in dislocation pile-up. Additionally, the densities of deformation twins and dislocations decrease and the interaction between deformation twins and dislocations weakens with temperature. Thus, flow stress decreases with temperature either at 10^{-3} or 700 s^{-1} .

4 Discussions

4.1 Calculation of SFE

For fcc metals and alloys, twinning can be assumed that stacking faults (SFs) extend in parallel adjacent dense planes. According to calculation methods of SFE and thermodynamic data in Ref [2-4, 16], only Fe-Mn and Fe-Si excess terms are taken into account but the others involving the other element are neglected because of the little quantities considered, except for C element. The SFE calculation formulas are as follows:

$$\Gamma = 2\rho\Delta G^{\gamma\rightarrow\varepsilon} + 2\sigma^{\gamma/\varepsilon} \quad (1)$$

$$\Delta G^{\gamma\rightarrow\varepsilon} = \sum_i x_i \Delta G_i^{\gamma\rightarrow\varepsilon} + x_{Fe} x_{Mn} [C + D(x_{Fe} - x_{Mn})] + x_{Fe} x_{Si} [E + F(x_{Fe} - x_{Si})] \\ + a(1 - e^{-bx_C}) + cx_C x_{Mn} + \Delta G_{mg}^{\gamma\rightarrow\varepsilon} \quad (2)$$

where ρ is the molar surface density of atoms in the $\{1\ 1\ 1\}$ planes, $\sigma^{\gamma/\varepsilon}$ is the energy per surface unit of a $\{1\ 1\ 1\}$ interface between γ and ε , $\Delta G^{\gamma\rightarrow\varepsilon}$ the free molar enthalpy of the transformation $\gamma\rightarrow\varepsilon$, x_i the molar fraction of element i ($i=Fe, Mn, C, Al, Si$), $\Delta G_i^{\gamma\rightarrow\varepsilon}$ the free molar enthalpy of martensite formation, and $\Delta G_{mg}^{\gamma\rightarrow\varepsilon}$ a magnetic term due to the Neel transition of each phase. Based on the formulas and present data, SFE values of Fe-30Mn-3Si-4Al TWIP steel are 30, 63, 96, 128, 145 mJ/m^2 at 298, 573, 773, 973 and 1073 K respectively.

4.2 Analysis of deformation mechanism

Deformation mechanism and mechanical properties of fcc metals and alloys are related to the SFE. However, the SFE is influenced by temperature and chemical composition. There are some researches on relation between deformation mechanism and the SFE. Dumay et al. [4] found that for $10 \text{ mJ/m}^2 \leq \Gamma \leq 12 \text{ mJ/m}^2$, ε -martensite and α' -martensite occur while for $15 \text{ mJ/m}^2 \leq \Gamma \leq 17 \text{ mJ/m}^2$, only ε -martensite occurs by researching Fe-C-Mn-Cu serial steels after tension in quasi-static condition. Under quasi-static or static condition, Allain et al. [2] researched Fe-Mn-C austenitic alloys and

found that for $\Gamma < 18 \text{ mJ/m}^2$, ε -martensite transformation occurs while for $12 \text{ mJ/m}^2 < \Gamma < 35 \text{ mJ/m}^2$, deformation twinning occurs; Wang et al. [3] studied Fe-25Mn-3Si-3Al TWIP steel and discovered that for $21 \text{ mJ/m}^2 \cong \Gamma \cong 34 \text{ mJ/m}^2$, deformation twinning is the main deformation mechanism, while for $34 \text{ mJ/m}^2 < \Gamma < 76 \text{ mJ/m}^2$, the competition between deformation twinning and dislocation gliding is the main deformation mechanism, while for $\Gamma \cong 76 \text{ mJ/m}^2$, dislocation gliding is the main deformation mechanism. In a word, deformation mechanism is controlled by the SFE.

In this paper, effect of the SFE and strain rate on deformation mechanism of Fe-30Mn-3Si-4Al TWIP steel is studied. At 10^{-3} s^{-1} , there are many deformation twins at 298 K and twinning is the main deformation mechanism according to Figure 2 and Ref [3] while the density of deformation twins decreases a lot at 573 and 773 K, and the competition between twinning and dislocation gliding is the main deformation mechanism. With temperature up to 973 and 1073 K, there are no deformation twins and dislocation gliding is the main deformation mechanism. According to calculation of SFE values at different temperatures, at 10^{-3} s^{-1} , for $\Gamma \cong 30 \text{ mJ/m}^2$ at 298 K, twinning is the main deformation mechanism while for $30 \text{ mJ/m}^2 < \Gamma < 128 \text{ mJ/m}^2$ between 573 and 773 K, the competition between twinning and dislocation gliding is the main deformation mechanism, while for $\Gamma \cong 128 \text{ mJ/m}^2$, dislocation gliding is the main deformation mechanism above 973 K.

With strain rate increasing from 10^{-3} to 700 s^{-1} , twinning is the main deformation mechanism at 298 K according to Figure 3a while the density of deformation twins decreases at 573 K, but twinning is also the main deformation mechanism according to Figure 3b and Figure 5b. With temperature up to 773 and 973 K, the density of deformation twins is small as illustrated in Figure 3c and 3d and there are also dislocation cells and subgrains respectively as shown in Figure 4c and 3d, thus the competition between twinning and dislocation gliding is the main deformation mechanism. At 1073 K, deformation twins are very seldom and develop partially as shown in Figure 5e, thus dislocation gliding is the main deformation mechanism. According to calculation of SFE values at different temperatures, at 700 s^{-1} , for 30

$mJ/m^2 \cong \Gamma \cong 163 \text{ mJ/m}^2$ between 298K and 573K, twinning is the main deformation mechanism, while for $63 \text{ mJ/m}^2 < \Gamma < 145 \text{ mJ/m}^2$ between 773 and 973 K, the competition of twinning and dislocation gliding is the main deformation mechanism, while for $\Gamma \cong 145 \text{ mJ/m}^2$ above 1073K, dislocation gliding is the main deformation mechanism.

Based on data in Ref [2-4] and this paper, the effect of the SFE and strain rate on deformation mechanism is concluded as shown in Table 1. As can be seen, deformation mechanism changes from twinning to dislocation gliding with increasing the SFE. With strain rate increasing from 10^{-3} to 700 s^{-1} , the range of the SFE shifts forwards and increases for the same deformation mechanism. For instance, when twinning is the main deformation mechanism, for $21 \text{ mJ/m}^2 \cong \Gamma \cong 34 \text{ mJ/m}^2$, $\Delta\Gamma=13 \text{ mJ/m}^2$ in quasi-static or static condition while for $30 \text{ mJ/m}^2 \cong \Gamma \cong 63 \text{ mJ/m}^2$, $\Delta\Gamma=33 \text{ mJ/m}^2$ at 700 s^{-1} in high strain rate condition. The maximum SFE for twinning increases from $\Delta\Gamma=128 \text{ mJ/m}^2$ in quasi-static or static condition to $\Delta\Gamma=145 \text{ mJ/m}^2$ at 700 s^{-1} in high strain rate condition. In conclusion, increasing strain rate can extend the value range of SFE for twinning. The effect of strain rate coupling the SFE on deformation mechanism needs to study further in future.

5 Conclusions

Compression experiments were conducted between 298 and 1073 K at 10^{-3} and 700 s^{-1} respectively. Microstructures were observed. According to calculation of the SFE values at different temperatures, effect of SFE and strain rate on deformation mechanism was analyzed. Results are as follows:

- (1) Flow stress of Fe-30Mn-3Si-4Al TWIP steel decreases with temperature increasing from 298 to 1073 K at either 10^{-3} or 700 s^{-1} . Dynamic recovery is enhanced, and the densities of deformation twins and dislocations decrease with temperature.
- (2) At 10^{-3} s^{-1} , for $\Gamma \cong 30 \text{ mJ/m}^2$, twinning is the main deformation mechanism while for $30 \text{ mJ/m}^2 < \Gamma \cong 128 \text{ mJ/m}^2$, the competition between twinning and dislocation

gliding is the main deformation mechanism, while for $\Gamma \cong 128 \text{ mJ/m}^2$, dislocation gliding is the main deformation mechanism above 973 K.

- (3) At 700 s^{-1} , for $30 \text{ mJ/m}^2 \cong \Gamma \cong 63 \text{ mJ/m}^2$, twinning is the main deformation mechanism, while for $63 \text{ mJ/m}^2 < \Gamma < 145 \text{ mJ/m}^2$, the competition of twinning and dislocation gliding is the main deformation mechanism, while for $\Gamma \cong 145 \text{ mJ/m}^2$ above 1073K, dislocation gliding is the main deformation mechanism.
- (4) The SFE range for twinning is extended and shifted forwards by increasing strain rate.

References:

- [1] O. Grässel, G. Frommeyer, C. Derder, H. Hofmann, Phase transformation and mechanical properties of Fe-Mn-Si-Al TRIP steel, J. Phys. IV France C5 (1977) 383-388.
- [2] S. Allain, J.-P. Chateau, O. Bouaziz, S. Migot, N. Guelton, Correlations between the calculated stacking fault energy and the plasticity mechanisms in Fe–Mn–C alloys, Mater. Sci. Eng. A 387–389 (2004) 158-162.
- [3] S.H Wang, Z.Y Liu, W.N Zhang, G.D Wang, Investigations on temperature dependence of mechanical properties and the deformation mechanism of a TWIP steel, Acta Metall. Sin. 45 (2009) 573-578.
- [4] A. Dumay, J.-P. Chateau, S. Allain, S. Migot, O. Bouaziz, Influence of addition elements on the stacking-fault energy and mechanical properties of an austenitic Fe–Mn–C steel, Mater. Sci. Eng. A 483-484 (2008) 184-187.
- [5] X.Q Li, A. Almazouzi, Deformation and microstructure of neutron irradiated stainless steels with different stacking fault energy, J. Nucl. Mater. 385 (2009) 329-333.
- [6] S. Curtze, V.-T. Kuokkala, Dependence of tensile deformation behavior of TWIP steels on stacking fault energy, temperature and strain rate, Acta Mater. 58 (2010) 5129-5141.
- [7] Y. Zhang, N.R. Tao, K. Lu, Effects of stacking fault energy, strain rate and

temperature on microstructure and strength of nanostructured Cu–Al alloys subjected to plastic deformation, *Acta Mater.* 59 (2011) 6048-6058.

[8] V.S. Sarma, J. Wang, W.W. Jian, A. Kauffmann, H. Conrad, J. Freudenberger, Y.T. Zhu, Role of stacking fault energy in strengthening due to cryo-deformation of FCC metals, *Mater. Sci. Eng. A* 527 (2010) 7624-7630.

[9] A. E. Ehab, A.M. Ayman, S.S. Mahmoud, Role of stacking fault energy on the deformation characteristics of copper alloys processed by plane strain compression, *Mater. Sci. Eng. A* 528 (2011) 7579-7588.

[10] A.M. Lennon, K.T. Ramesh, A technique for measuring the dynamic behavior of materials at high temperatures, *Int. J. Plasticity* 14 (1998) 1279-1292.

[11] J.A. Jiménez, G. Frommeyer, Analysis of the microstructure evolution during tensile testing at room temperature of high-manganese austenitic steel, *Mater. Charact.* 61 (2010) 221-226.

[12] D.Z. Li, Y.H. Wei, C.Y. Liu, L.F. Hou, D.F. Liu, X.Z. JIN, Effects of High Strain Rate on Properties and Microstructure Evolution of TWIP Steel Subjected to Impact Loading, *J. Iron Steel Res. Int.* 17 (2010) 67-73.

[13] S. Vercammen, B. Blanpain, B.C. De Cooman, P. Wollants, Cold rolling behaviour of an austenitic Fe-30Mn-3Al-3Si TWIP steel: the importance of deformation twinning, *Acta Mater.* 52 (2004) 2005-2012

[14] Z.L. Mi, D. Tang, Y.J. Dai, H.T. Jiang, J.C. Lü. In-situ observation on the deformation behaviors of Fe-Mn-C TWIP steel, *Int. J. Miner. Metall. Mater.* 16 (2009) 646-649.

[15] C.X. Huang, K. Wang, S.D. Wu, Z.F. Zhang, G.Y. Li, S.X. Li, Deformation twinning in polycrystalline copper at room temperature and low strain rate, *Acta Mater.* 54 (2006) 655-665.

[16] L. Li, T. Y. Hsu, Gibbs free energy evaluation of the fcc (γ) and hcp (ϵ) phases in Fe-Mn-Si alloys, *Calphad* 21 (1997) 443-448.

Table captions:

Table 1 Effect of SFE and strain rate on deformation mechanism

Figure captions:

Figure 1 True strain-stress curves under different temperatures at (a) 10^{-3} s^{-1} and (b) 700 s^{-1}

Figure 2 Microstructures under different temperatures at 10^{-3} s^{-1} : (a) 298K; (b) 573 K; (c) 773 K; (d) 973 K; (e) 1073 K

Figure 3 Microstructures under different temperatures at 700 s^{-1} : (a) 298K; (b) 573 K; (c) 773 K; (d) 973 K; (e) 1073 K

Figure 4 Dislocation configurations under different temperatures at 700 s^{-1} : (a) 298K; (b) 573K; (c) 773K; (d) 973K

Figure 5 Deformation twins under different temperatures at 700 s^{-1} : (a) 298 K; (b) 573 K; (c) 773 K; (d) 973 K; (e) 1073 K

Table 1

Deformation mechanism	α' 和 ε -martensite	ε -martensite	twinning	gliding and twinning	gliding
SFE/mJ/m ² (quasi-static)	$10 \cong \Gamma \cong 12$	$12 < \Gamma \cong 18$	$21 < \Gamma \cong 34$	$34 < \Gamma < 128$	$\Gamma \cong 128$
SFE/mJ/m ² (700 s ⁻¹)	--	--	$30 \cong \Gamma \cong 63$	$63 < \Gamma < 145$	$\Gamma \cong 145$